Electrochemical and Solid-State Letters, **8** (6) B21-B24 (2005)
1099-0062/2005/8(6)/B21/4/$7.00 © The Electrochemical Society, Inc.

In Situ Investigation of Localized Corrosion of Aluminum Alloys in Chloride Solution Using Integrated EC-AFM/SECM Techniques

A. Davoodi,[a] J. Pan,[a,*,z] C. Leygraf,[a,*] and S. Norgren[b]

[a]*Department of Materials Science and Engineering, Royal Institute of Technology, SE-100 44 Stockholm, Sweden*
[b]*Sapa Technology, SE-612 81 Finspång, Sweden*

Scanning electrochemical microscopy (SECM) has been integrated with electrochemical atomic force microscopy (EC-AFM), and applied for *in situ* studies of localized corrosion of Al alloys in NaCl solution. The instrument utilizes a dual mode probe, which functions both as a normal cantilever and as an ultramicroelectrode. The I^-/I_3^- redox mediator was used for mapping of local electrochemical current. Concurrent topography and electrochemical activity maps have been obtained on the same surface area with micrometer lateral resolution. Preliminary results show ongoing localized dissolution related to intermetallic particles in the Al alloys, which may occur well below the breakdown potential.
 [DOI: 10.1149/1.1911900]

Manuscript submitted January 18, 2005; revised manuscript received March 2, 2005. Available electronically April 21, 2005.

Due to the complexity of the microstructure of multi-component Al alloys, the mechanism of localized corrosion of Al alloys is still not completely understood, especially regarding the influence of various kinds of intermetallic precipitates in the alloys. Further studies are needed on formation of pits at intermetallic compounds and deterministic factors in pit initiation, *e.g.*, second phase particle size, aspect ratio, chemistry, and the conditions of pit formation.[1,2] The studies of intermetallic precipitates require high-lateral-resolution *in situ* techniques that can resolve particles of micrometer or submicrometer sizes in aqueous solutions. In this context, different local techniques have been employed during the last decade, *e.g.*, atomic force microscopy (AFM), scanning electrochemical microscopy (SECM), near-field scanning optical microscopy (NSOM), and confocal laser scanning microscopy (CLSM). Scanning Kelvin probe force microscopy (SKPFM), an *ex situ* technique, has also been shown capable to provide useful complementary information.

AFM, used in air or in solution under electrochemical potentiostatic control, has been employed *in situ* and *ex situ* to study the role of Fe-rich intermetallic precipitates such as Al_3Fe on local dissolution of Al-6061 in aerated NaCl solution.[3] The *in situ* imaging of the topography showed formation of cavities at open-circuit potential and cavity growth around the intermetallic precipitates. SECM, able to map variations in local electrochemical activity,[4-6] has been used to study pitting corrosion around MnS inclusions in stainless steels in NaCl solution, using carbon fiber SECM tip and I^-/I_3^- as the redox mediator.[7] SECM was also utilized to spatially resolve the heterogeneous cathodic activity at AA2024 surfaces, using Pt microelectrode and [$(DMAFc^+$, $Fe^{2+}/DMAFc^{2+}$, Fe^{3+}] redox mediator.[8] The SECM images showed locally high redox reactivity that was attributed to intermetallic particles. However, in these reports, the resolution of current mapping was quite poor as seen from the blurred SECM images.

NSOM, using tuning-fork control and specially fabricated tips to obtain high-resolution topography, has been used in combination with fluorescent dye, fluorescence microscopy, and SECM, to study localized corrosion behavior of AA2024.[9,10] The anodic dissolution sites were identified by the fluorescent dye, and deposition of ring-like corrosion products (aluminum oxyhydroxides) around intermetallic particles was observed both at open-circuit potential and under anodic polarization. CLSM, a contact-free method for sharp imaging of sample surface, has been applied to study *in situ* the corrosion attack at and around intermetallic particles in AA2024 in different solutions, *e.g.*, trench formation next to cathodic intermetallic particles.[11,12] Galvanic coupling between the matrix and the intermetallic particles was found to control the attack rates. It was also shown that not every cathodic intermetallic particle developed trenches.

SKPFM, an AFM-based technique for mapping Volta potential variation over sample surface, has been used to investigate corrosion tendency associated to intermetallic particles in Al alloys.[13,14] The results provide good understanding of local corrosion phenomena and can be used for prediction of local corrosion sites. However, because the Volta potential gives only "practical nobility", the interpretation should be careful and backed up by local electrochemical data and composition and morphology information.

In this paper, we present the application of an integrated EC-AFM and SECM system for *in situ* study of localized corrosion of Al alloys in solutions. The system is capable of obtaining simultaneous topographic and electrochemical activity information of the same surface area. By using a dual mode cantilever/tip, the AFM-based SECM has a high lateral resolution (better than normal SECM) and able to reveal local dissolution sites. This integrated EC-AFM/SECM technique has recently been introduced for characterization of Ti/TiO_2/noble metal anodes,[15] and for mapping of enzyme activity[16] and biosensor surfaces.[17] The critical issue in this approach is to fabricate a dual mode cantilever/tip, which acts as the cantilever for the AFM and also the micro- or nanoelectrode tip for the SECM as well. To our knowledge, this is the first time the integrated EC-AFM/SECM was applied for *in situ* studies of localized corrosion of Al alloys.

Experimental

Sample.—Samples of commercial Al alloys AA1050 (Al, 0.31% Fe, 0.06% Si, 0.01% Mn, 0.01% Mg, 0.01% Zn, 0.01% Ti), and AA3003 (Al, 0.43% Fe, 0.13% Si, 1.0% Mn, 0.01% Mg, 0.01% Zn, 0.02% Ti), in 0.4 mm thick sheet form, were provided by Sapa Technology, Sweden. The intermetallic components are mainly Al_3Fe and AlFeSi-type phases in the AA1050, and $Al_6(Mn,Fe)$ and α-$Al_{12}(Mn,Fe)_3Si_{(1-2)}$ in AA3003, respectively. For *in situ* AFM/SECM measurements, the strip sample was fixed vertically on a brass base by conducting adhesive (for electrical connection), then mounted in a low viscosity epoxy leaving 0.02 cm^2 exposed surface area facing upward. The samples were carefully prepared, and no crevice corrosion was observed in the measurements. The investigated surface was in longitudinal crosssection. The surface was mechanically ground with SiC paper up to 4000 grit, then polished with 1 and 0.25 μm diamond pastes, respectively. 99.5 vol % ethanol was used during the polishing steps.

Solutions.— Reagent NaCl and KI and distilled water were used to make up the solution. The NaCl concentration was 10 mM, and

* Electrochemical Society Active Member.
z E-mail: jinshanp@kth.se

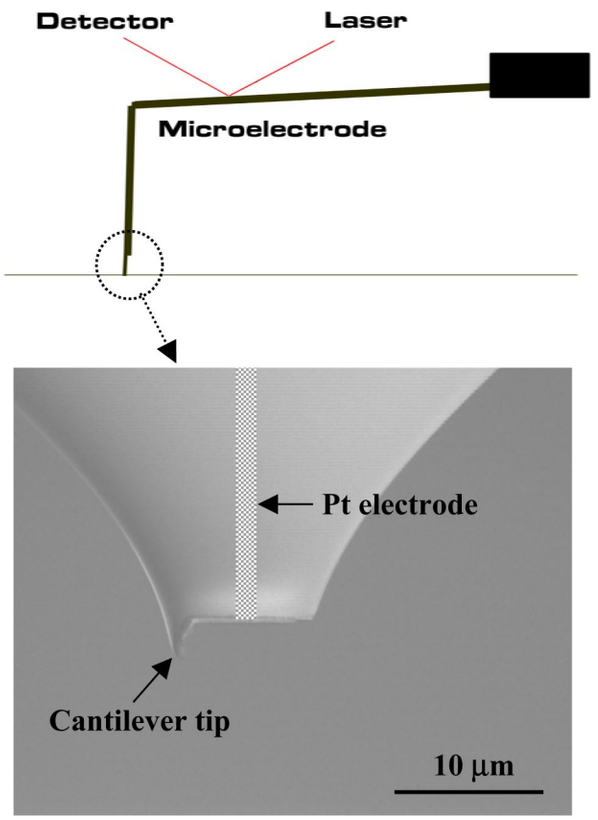

Figure 1. Scheme of integrated EC-AFM/SECM probe and micrograph of the tip end.

KI was added as the redox mediator for SECM mapping of electrochemical current due to the local corrosion process. The solution was aerated in all the experiments.

Electrochemical cell.—The electrochemical cell made of Teflon was used for the EC-AFM/SECM measurements. When 5 cm^3 of solution was added, the solution layer covering the sample surface had a thickness of ~3 mm. A saturated Ag/AgCl was used as the reference electrode, and a Pt foil surrounding the sample as the counter electrode.

Instruments.— Cyclic polarization of the Al alloy samples was carried out using an EG&G Potentiostat/Galvanostat model 273A. All potential values are given herein with respect to the Ag/AgCl reference electrode. The voltammogram of the ultramicroelectrode was characterized by using the iProbe potentiostat, as described below.

The EC-AFM/SECM instrument used was a Resolver (Quesant, USA), equipped with the iProbe package and the dual mode cantilever/tip probe, supplied by Windsor Scientific Ltd., UK. The iProbe package includes a battery-driven, low-noise and high-sensitivity (pico-A) bipotentiostat for separate control of the potential of the sample and the tip, and for measurement of the total current through the counter electrode and the local current though the tip. The dual mode probe is a "L" shaped microelectrode (Fig. 1). The arm is flattened and coated with gold for laser reflection. The bending part is insulated with epoxy and its end was cut with focused ion beam (FIB) to produce a disk electrode with the core Pt electrode size about 1-5 um and the disk size about 10 um. A small tip is built out of the epoxy with FIB on the disk beside the core Pt electrode to act as the AFM tip, Fig. 1. In the integrated EC-AFM/SECM measurement, the first line scan is a normal AFM operation in contact mode and a line of surface profile was collected. Then the feedback is stopped and the tip is withdrawn to a preset distance (a few 100 nm to a few μm) from the surface, and in the second line scan the tip follows the surface profile obtained from the first scan, and collects the local current using a redox couple as mediator. By scanning over the surface in such a way, concurrent AFM topography and SECM current distribution are obtained on exactly the same area. The distance between the sample and the tip for the SECM mapping is kept constant, hence the lateral resolution is maintained the same during the mapping. Depending on the scan speed (frequency), it takes a few minutes to acquire a pair of AFM and SECM images, roughly twice so long as when only AFM imaging.

In this work the SECM was performed in sample-generator and tip-collector mode, using I^-/I_3^- couple as the redox mediator, as described below. The sample was anodically polarized and localized corrosion (anodic dissolution) started to occur at certain sites on the Al alloy surface, where the redox reduction also occurred, probably as

$$Al \Rightarrow Al^{3+} + 3e^- \quad [1]$$

$$I_3^- + 2e^- \Rightarrow 3I^- \quad [2]$$

Meanwhile, the tip was controlled at a potential at which the redox oxidation occurs at the maximum current density limited by diffusion of I^- ions towards the tip

$$3I^- \Rightarrow I_3^- + 2e^- \quad [3]$$

By this arrangement, local high electrochemical current of the Al alloy surface will be detected due to the high redox oxidation current at the tip, as a result of increased redox reduction current at the dissolution sites on the Al alloy surface. The lateral resolution of the SECM depends on the tip size, the sample-tip distance and the electrolyte conductivity. The tip at the endpoint creates a little gap between conductive core electrode and sample. This gap avoids short circuit between the electrode and the sample, and ensures that the tip collects only electrochemical activity on the sample surface. The integrated EC-AFM/SECM system was calibrated by simultaneous AFM and SECM imaging of patterned Au bends on a Si wafer in the electrolyte.

Results and Discussion

Conventional cyclic polarization of large Al alloy samples (1 cm^2) in the solution was performed to determine the corrosion potential, current density in passive region and the breakdown potential values. These data provide background information useful for the EC-AFM/SECM experiments, for instance, for setting the polarization over-potential.

Cyclic voltammetry (CV) measurements of the dual mode EC-AFM/SECM probe were performed to obtain voltammograms of the redox couple on the Pt tip. Figure 2 shows the tip response when the 10 mM NaCl solution contains 0, 5, 10, and 50 mM KI, respectively. Without KI, there is no current peak between 0.0 and 1.0 V, *i.e.*, essentially no oxidation and reduction reaction occurring on Pt in this solution. With added KI, the reduction (Reaction 2) peak is clearly seen around or below 0.5 V, and the oxidation (Reaction 3) limiting currents appear above a certain potential depending on KI concentration. With 5 mM KI the tip exhibits stable limiting oxidation current, whereas at higher KI concentrations the tip current becomes noisy. Therefore, the 10 mM NaCl + 5 mM KI solution was chosen for the EC-AFM/SECM experiments. The open-circuit potential was −840 mV for AA1050 and −790 mV for AA3003, respectively, *vs.* Ag/AgCl electrode in the solution. The tip potential was normally controlled at 750 mV to ensure maximum collection of the local current.

The EC-AFM/SECM experiments have generated concurrent topographic images and electrochemical current maps, with satisfactory quality, showing details of the ongoing localized corrosion processes associated with intermetallic particles in the Al alloys. As an example, Fig. 3 displays results for AA1050 at a small anodic po-

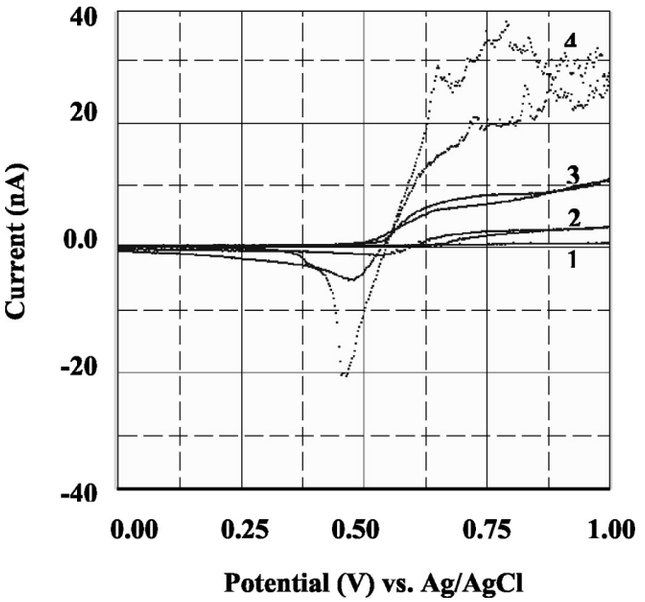

Figure 2. CVs of dual mode probe in 10 mM NaCl with different KI concentrations. Numbers 1-4 show tip response for 0, 5, 10, and 50 mM KI, respectively.

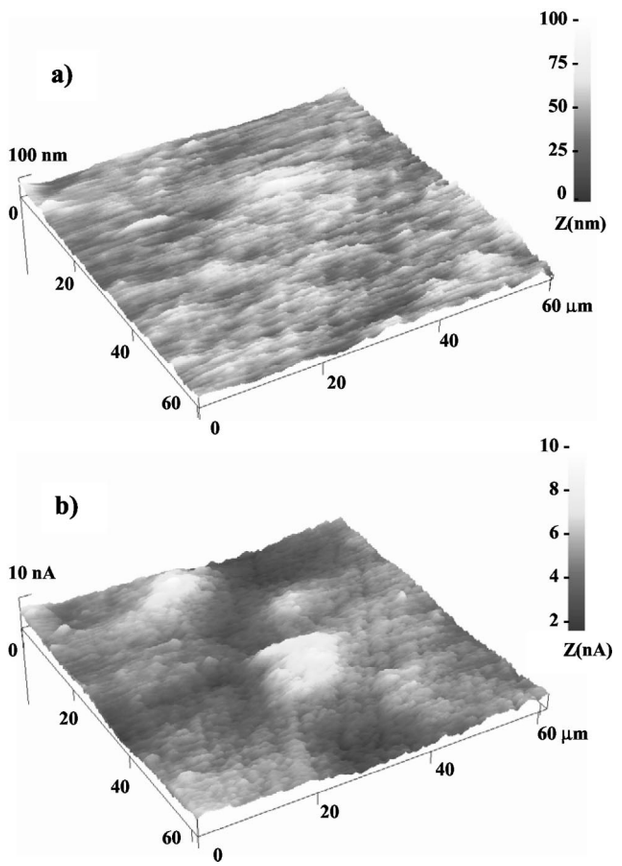

Figure 3. EC-AFM/SECM images of AA1050 in 10 mM NaCl + 5 mM KI at 50 mV anodic polarization, and tip at +750 mV *vs.* Ag/AgCl. (a) Topography and (b) electrochemical activity map.

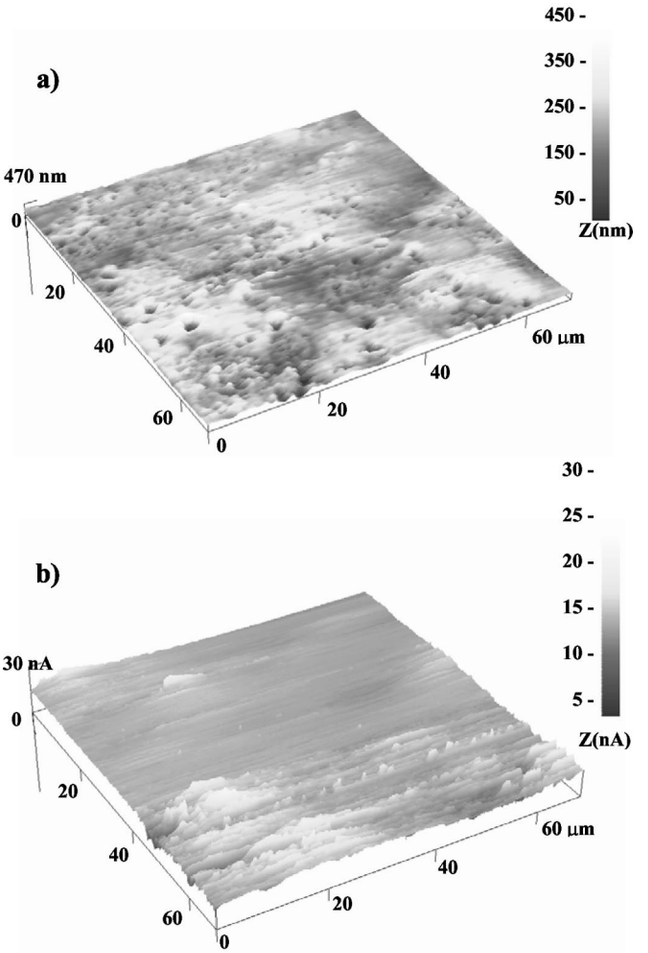

Figure 4. EC-AFM/SECM images of AA1050 in 10 mM NaCl + 5 mM KI at 300 mV anodic polarization (near breakdown potential), and tip at +750 mV *vs.* Ag/AgCl. (a) Topography and (b) electrochemical activity map.

larization (50 mV), with a scanned area of 60 x 60 μm. Although the surface was still very smooth as seen from small height variations (<100 nm) in the AFM topographic image, Fig. 3a, the SECM electrochemical current map showed enhanced current on local areas (lighter), Fig. 3b. The maximum current was about 10 nA. This high current area was ~10 μm in dimension, and could be related to an active site. Before any topographic change could be observed, the electrochemical mapping already revealed at least two local dissolution sites. Since the local current peaks were stable at least for several minutes (scanning time), these sites are regarded as likely precursors for localized corrosion, not short-life transient events.

When the AA1050 sample was anodically polarized 300 mV (near breakdown potential), the topography shows many small pits, Fig. 4a. The electrochemical current map, Fig. 4b, shows a higher background current compared to that for 50 mV anodic polarization. This is probably due to many active sites close to each other, so that the local current could not be resolved in the SECM mapping. However, in the later period of the scanning (lower part of the image), some high current (up to 30 nA) sites appeared in the SECM image. This might be related to developing pits or trenches on the surface.

Figure 5 shows concurrent AFM and SECM images obtained for AA3003 at 100 mV anodic polarization (passive region) in 10 mM NaCl + 5 mM KI solution. The maximum current was found to be about 14 nA in this case. Ignoring background details, the images clearly show two active sites exhibiting different local

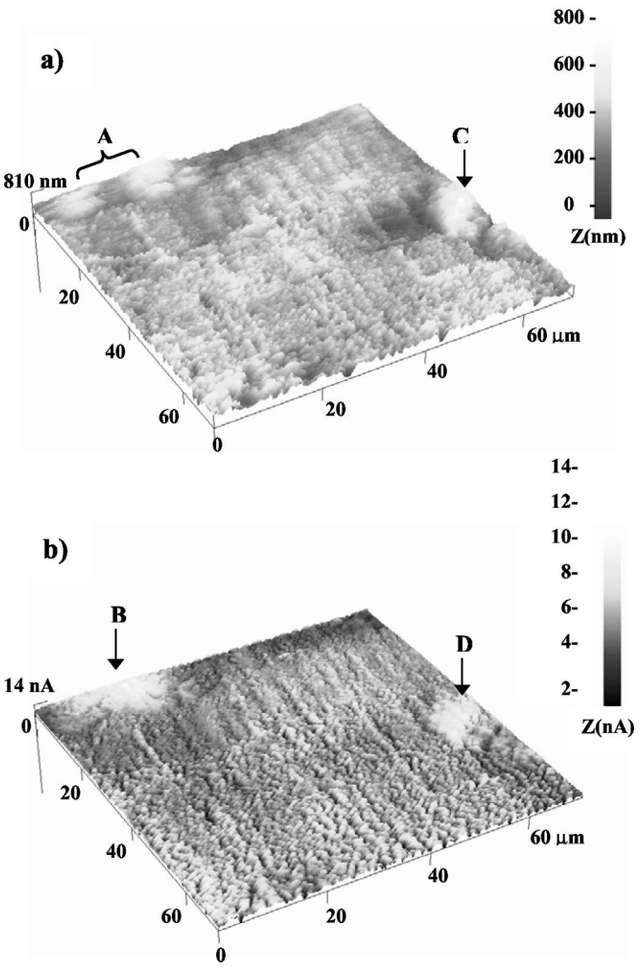

Figure 5. EC-AFM/SECM images of AA3003 in 10 mM NaCl + 5 mM KI at 100 mV anodic polarization, and tip at +750 mV *vs.* Ag/AgCl. (a) Topography and (b) electrochemical activity map.

corrosion behavior. At site A in Fig. 5a, deposition of corrosion products (apparently surrounding some particle) is clearly related to the high current area B in Fig. 5b, with the high current in between the deposits. On the other hand, the deposit at site C (Fig. 5a) appeared to be the same location as the local high current area D (Fig. 5b). In the former case, it is probably due to enhanced local dissolution of the Al alloy matrix at the boundary of a large intermetallic particle (because of a weaker passive film there), and consequent deposition of oxy-hydroxides around the particle as a result of local saturation of Al ions, as proposed for AA2024.[10,11] In the later case, pitting at some site was most likely initiated, resulting in local high current and also deposition of corrosion product over the pit. Both ring-like deposit of corrosion products surrounding large intermetallic particles and domelike corrosion products covering small pits have been observed by *in situ* AFM imaging of the samples using a standard cantilever with a better resolution (results to be published). It can be seen from the SECM images in this work, that the AFM-based SECM has a micrometer lateral resolution, which gives electrochemical current images significantly better than those reported previously.[8,11]

More experiments are ongoing to investigate localized corrosion of Al alloys related to different kinds of intermetallic particles.

Conclusions

The integrated EC-AFM/SECM has been shown to be a valuable technique for investigating the influence of intermetallic particles on localized corrosion of Al alloys. Concurrent AFM topographic images and SECM electrochemical current maps could be obtained *in situ*, with micrometer lateral resolution, providing detailed information of the localized dissolution associated with different kinds of intermetallic particles, and deposition of corrosion products surrounding large particles or covering small pits. Preliminary results have shown that enhanced local dissolution may occur well below the breakdown potential, but only a small fraction of particles is involved.

Acknowledgments

Sapa Heat Transfer AB, Finspång, Sweden, and the Brinell Centre at the Royal Institute of Technology, Stockholm, Sweden, are acknowledged for the financial support. Dr. Y. Zhu of Windsor Scientific Ltd. is greatly acknowledged for assistance with the instrument and the experiments, as well as for valuable discussion.

The Royal Institute of Technology assisted in meeting the publication costs of this article.

References

1. G. S. Frankel, *J. Electrochem. Soc.*, **145**, 2186 (1998).
2. Z. Szklarska-Smialowska, *Corros. Sci.*, **41**, 1743 (1999).
3. J. O. Park, C. H. Paik, Y. H. Huang, and R. C. Alkire, *J. Electrochem. Soc.*, **146**, 517 (1999).
4. A. J. Bard, F.-R. F. Fan, J. Kwak, and O. Lev, *Anal. Chem.*, **61**, 132 (1989).
5. J. Kwak and A. J. Bard, *Anal. Chem.*, **61**, 1221 (1989).
6. J. Kwak and A. J. Bard, *Anal. Chem.*, **61**, 1794 (1989).
7. C. H. Paik, H. S. White, and R. C. Alkire, *J. Electrochem. Soc.*, **147**, 4120 (2000).
8. J. C. Seegmiller and D. A. Buttry, *J. Electrochem. Soc.*, **150**, B413 (2003).
9. M. Büchler, J. Kerimo, F. Guillaume, and W. H. Smyrl, *J. Electrochem. Soc.*, **147**, 3691 (2000).
10. T. L. Knutson, F. Guillaume, W.-J. Lee, M. Alhoshan, and W. H. Smyrl, *Electrochim. Acta*, **48**, 3229 (2003).
11. G. O. Ilevbare, O. Schneider, R. G. Kelly, and J. R. Scully, *J. Electrochem. Soc.*, **151**, B453 (2004).
12. O. Schneider, G. O. Ilevbare, J. R. Scully, and R. G. Kelly, *J. Electrochem. Soc.*, **151**, B465 (2004).
13. V. Guillaumin, P. Schmutz, and G. S. Frankel, *J. Electrochem. Soc.*, **148**, B163 (2001).
14. J. H. W. de Wit, *Electrochim. Acta*, **49**, 2841 (2004).
15. J. P. G. de Mussy, J. V. Macpherson, and J. L. Delplanck, *Electrochim. Acta*, **48**, 1131 (2003).
16. C. Kranz, A. Kueng, A. Lugstein, E. Bertagnolli, and B. Mizaikoff, *Ultramicroscopy*, **100**, 127 (2004).
17. Y. Hirata, S. Yabuki, and F. Mizutani, *Bioelectrochemistry*, **63**, 217 (2004).